



An Experimental Evaluation of a Developed Flame Holder Supplied with Two Air Sources

Islam M. Mesallam¹, Ahmed A.A. Attia², Khairy H. El-Nagar³, Ismail M.M. ElSemary⁴

^{1,2,3,4}Combustion and Energy Technology Lab, Mechanical Engineering Department, Shoubra Faculty of Engineering, Benha University.

⁴Department of Mechanical Engineering, College of Engineering, Northern Border University, Arar, Saudi Arabia.

Abstract: In this study, a new developed flame holder which is designed as a double cone with three holes at the top cone to spout the fuel to the combustion zone has been investigated experimentally. The air and fuel have been supplied to the combustion area through a triple coaxial pipe. The inner pipe of the coaxial pipe delivers fuel, while the middle and outside pipes deliver primary and secondary air to the combustion zone, respectively. A conversion diversion channel is constructed on the primary air output to optimize air and fuel mixing by increasing turbulence in the primary air. The experiment was carried out in still air under atmospheric circumstances, using the diffusion flame concept. The results showed that mixing secondary and primary air in the combustion zone had an effect on flame temperatures, flame length, flame width, and emissions.

KEYWORDS: diffusion jet flame, Flame holder, Flame length, flame width, emissions

1. INTRODUCTION

Combustion is an essential source of energy in our everyday lives, and it may be employed for a variety of purposes in modern human life [1]. Combustion is a chemical reaction that occurs when a fuel is oxidized, resulting in the release of a huge amount of energy [2].

Diffusion flame is an essential flame mode because it is more relevant and connected to industry and household life than premixed flame mode. Diffusion flames are types of flames in which the oxidizer and fuel react directly in the combustion zone [3]. Flame jets are widely employed in industry because they provide considerable benefits in terms of energy savings, response time, and convective heat transfer [4]. The jet geometry is a valuable tool for improving the combustion performance of the flame jet [5][6].

M. Henriksen et al. examined the effect of nozzle geometry on the length of a hydrogen jet flame. The results showed changing the nozzle shape enhanced the length of the jet flame [7]. According to Changchun Liu et al., the shape of the flame holder influences flame stability, flame height, and flame lift off distance [8]. Toshio Mogi and Sadashige Horiguchi studied a hydrogen jet diffusion flame and a circular nozzle with different diameters were used. The results show that the aspect ratio has an impact on the flame size [9].

Because flame stability is important for the flame jet in industries, several researches have been done to examine flame stability, length, and lift off distance of the flame jet [10][11][12][13]. Stephen R. Turns stated that the closer the flame is to the flame nozzle, the more stable the flame will be, but the overheating of the burner is unavoidable [14]. Halleh Mortazavi et al. investigated the

addition of carbon dioxide to methane in diffusion flame combustion. The results revealed that when the carbon dioxide level increased, the flame temperature and soot generation dropped, while the flame duration increased (Halleh Mortazavi, Yiran Wang, Zhen Ma, Yang Zhang, 2018).

2. Experimental setup

The experimental setup was made up of a burner, which consists of a triple coaxial pipe that used to convey fuel and air to the combustion area. The inner pipe diameter was 3 mm and the thickness was 1.5 mm, and it was utilized to transfer fuel to the combustion zone.

The middle pipe was made of steel with an inner diameter of 30 mm and a thickness of 3 mm, and it was used to transport primary air to the combustion zone. The outer pipe, made of Pyrex glass with an inner diameter of 52 mm and a thickness of 3 mm, was employed to carry secondary air to the combustion zone. A conversion diversion path, as shown in Figure 1, was installed at the top of middle pipe to enhance air turbulence in the combustion area. The new design of flame holder, as shown in Figure 2, is located inside the conversion diversion channel and has a double cone form with an outside diameter of 21 mm and three circular fuel ports.

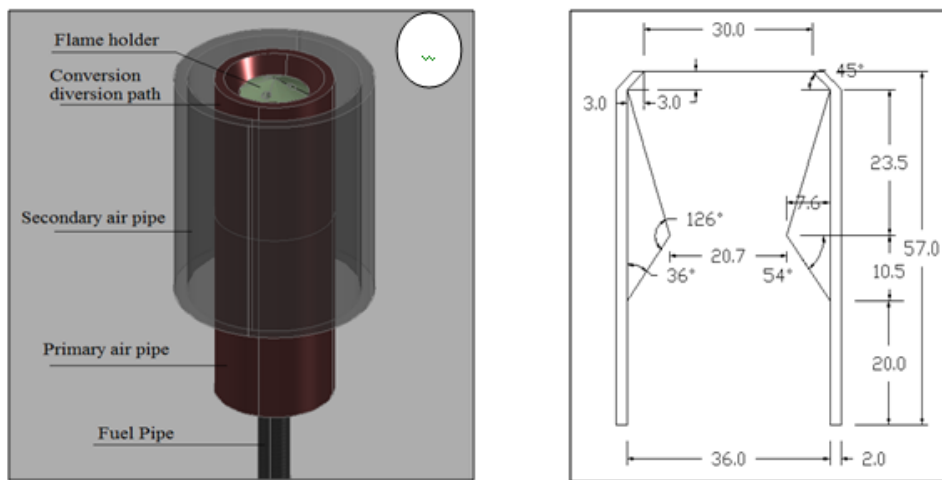


Figure 1 The burner parts construction (a) Burner parts, (b) conversion diversion path (dimensions in mm).

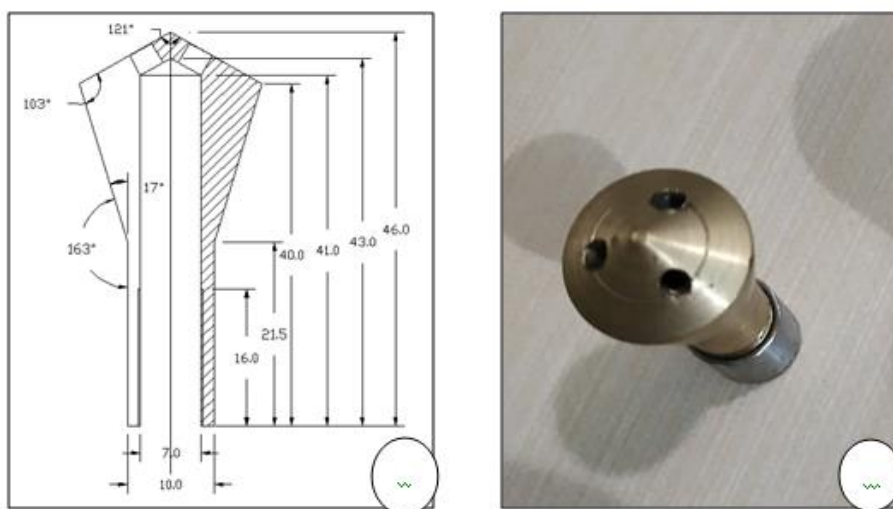


Figure 2 The bluff-body construction (a) flame holder design (dimensions in mm), (b) flame holder photo.

In this experimental investigation, natural gas was used as the fuel and the amount of fuel Q_f was set to a fixed value throughout the

experiment $Q_f = 2.398 \times 10^{-5} \text{ m}^3/\text{s}$. The volumetric composition and properties of natural gas is shown in table 1.

Table 1: the volumetric composition of Natural gas.

Composition	Component	Formula	Volume %
	Methane	CH_4	84.9 – 94.82
	Ethane	C_2H_6	3.12 – 7.1
	Propane	C_3H_8	1.09 – 2.6
	Iso-Butane	C_4H_{10}	0.04 – 0.5
	n-Butane	C_4H_{10}	0.02 – 0.65
	Iso-Pentane	C_5H_{12}	0.01 – 0.2
	n-Pentane	C_5H_{12}	0.02 – 0.14
	Hexane's plus	C_6H_{14}	0.04 – 0.11
	Nitrogen	N_2	0.11 – 0.3
	Carbon dioxide	CO_2	0.7 – 3.5
Properties	Calorific Value		42852 kJ/kg
	Density		0.754 kg/m ³
	Correct (A/F)		17.2
	Molecular weight		18.87

Thermocouples S-Type (Platinum – Platinum Radium 10 %) were used to measure the flame temperatures in the combustion area and the positions of the thermocouples are shown in Figure 3. The positions of thermocouples of each run contain five levels to measure the temperatures of the flames. The difference in height between each level is 15 mm and each level has three horizontal measuring points with a 10 mm difference between them.

The flames were captured on video and converted to photographs using computer software, which were then used by MATLAB and AutoCAD to determine the flames' length and width. The MATLAB is used for photo processing to determine the edges of each photo and AutoCAD is used to determine the length and width of the flame. The concentrations of CO (ppm) and NO_x (ppm) were determined using an exhaust analyzer (optima 7) as shown in Figure 4.

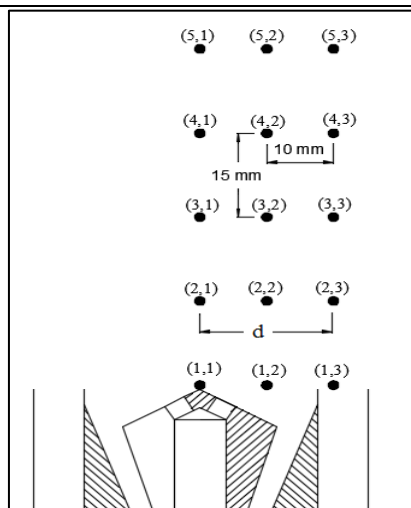


Figure 3 thermocouples measuring positions



Figure 4 exhaust gas analyzer optima 7

3.Results and discussion

The flame holder is located at the top of the burner, and the impact of changing air velocity on combustion performance was studied by keeping primary air velocity (V_2) constant while changing the secondary air velocity (V_1).

3.1Flame temperatures

Figure 5 show the distribution of flame temperatures for primary air velocity (V_2) =

14.55 m/s, with different secondary air velocities (V_1). The results showed that the highest temperature was 314.1 °C at $T_{2,1}$ and 274.7 °C at $T_{1,1}$ when the secondary air velocity V_1 was 6.95 m/s. Also, when the secondary air velocity V_2 was 0, the resulted temperatures were 205.5 °C at $T_{2,1}$ and 306.7 °C at $T_{1,1}$, indicating that the presence of secondary air had an effect on the flame temperatures.

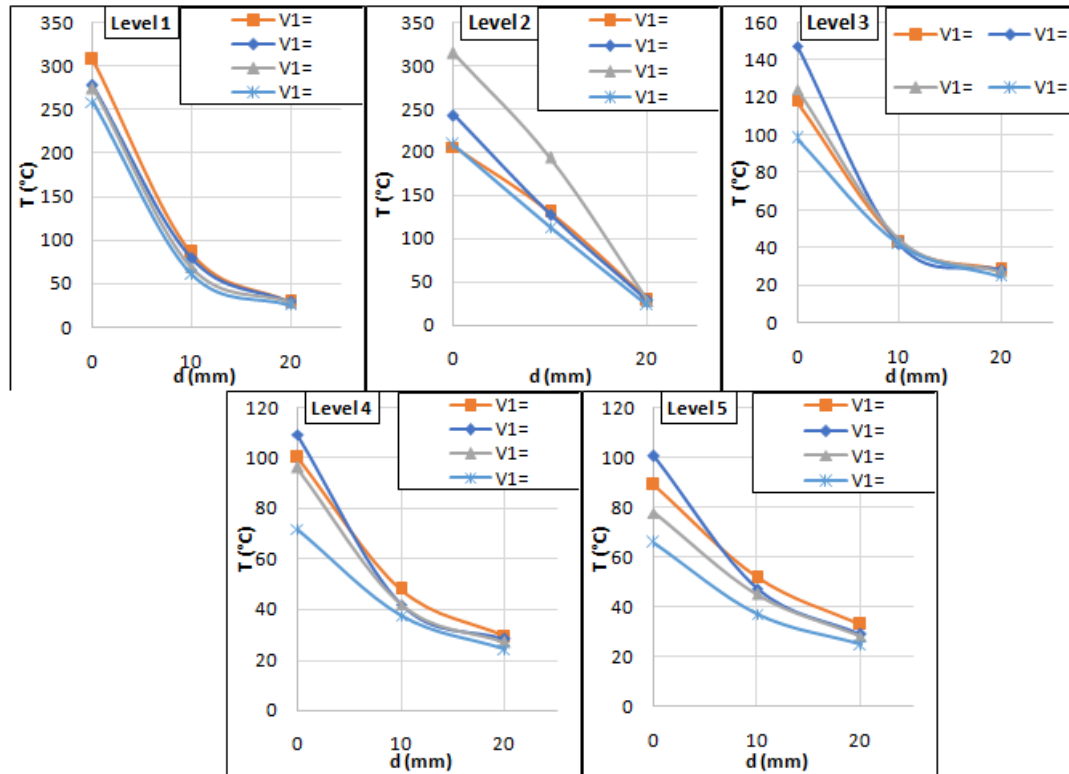


Fig 5: the effect of changing the secondary air velocity on temperature profile at fixed primary air velocity ($V_2 = 14.55$ m/s).

The primary air velocity was increased to 16.5 m/s and maintained at that value, while different secondary air velocities were supplied to the combustion zone. Figure 6 show the distribution of flame temperature at primary air velocity (V_2) = 16.5 m/s, with different secondary air velocity (V_1). The results show that when secondary air velocity was 0, the flame temperature at $T_{1,1}$ reached 269.3 °C and $T_{2,1}$ reached 400.9 °C, but when the secondary

air velocity increased to 6.17 m/s, the flame temperature at $T_{1,1}$ increased to 300.4 °C and $T_{2,1}$ reduced to 294.3°C. Also, when the secondary air velocity increased to 6.6 m/s, the flame temperature at $T_{1,1}$ increased to 406.5 °C and $T_{2,1}$ reduced to 227.8°C and when the secondary air velocity increased to 9.22 m/s, the flame temperature at $T_{1,1}$ was 405 °C and $T_{2,1}$ increased to 406.8°C.

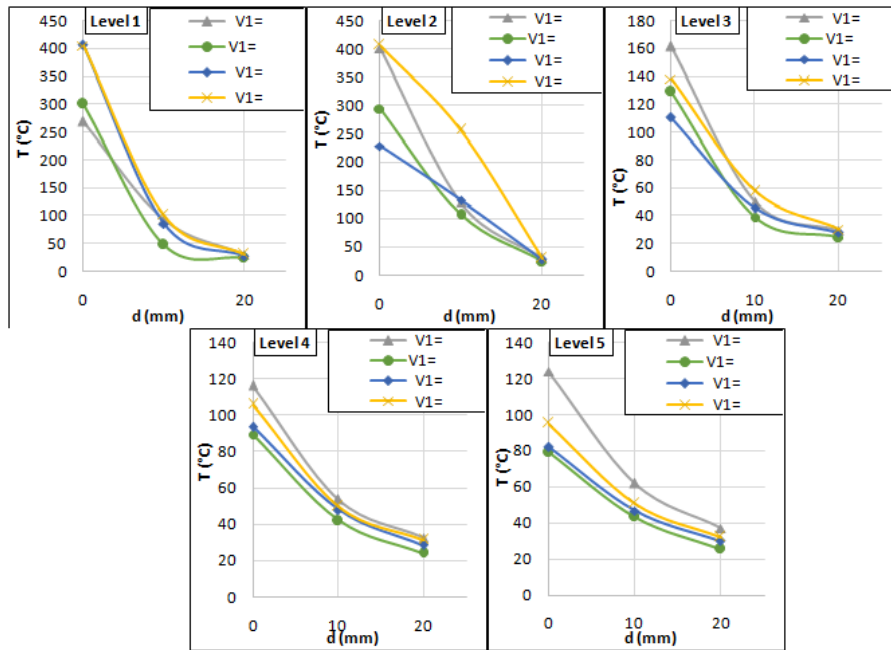


Fig 6: the effect of changing the secondary air velocity on temperature profile at fixed primary air velocity ($V_2 = 16.5$ m/s).

The primary air velocity was increased to 17.94 m/s and maintained at that value, while the combustion zone was supplied with various secondary air velocities. Figure 7 shows that the flame temperature distribution at primary air velocity (V_2) = 17.94 m/s, with different secondary air velocity (V_1). The results show that when secondary air velocity was 6.19 m/s, the flame temperature at $T_{1,1}$ reached 308.3 °C and $T_{2,1}$ reached 339 °C, and when the

secondary air velocity increased to 6.92 m/s, the flame temperature at $T_{1,1}$ was 302.9 °C and $T_{2,1}$ reduced to 277.5 °C. Also, when the secondary air velocity increased to 7.27 m/s, the flame temperature at $T_{1,1}$ decreased to 262.9 °C and $T_{2,1}$ increased to 305.7 °C and when the secondary air velocity increased to 8.35 m/s, the flame temperature at $T_{1,1}$ was 318.5 °C and $T_{2,1}$ increased to 296.2 °C.

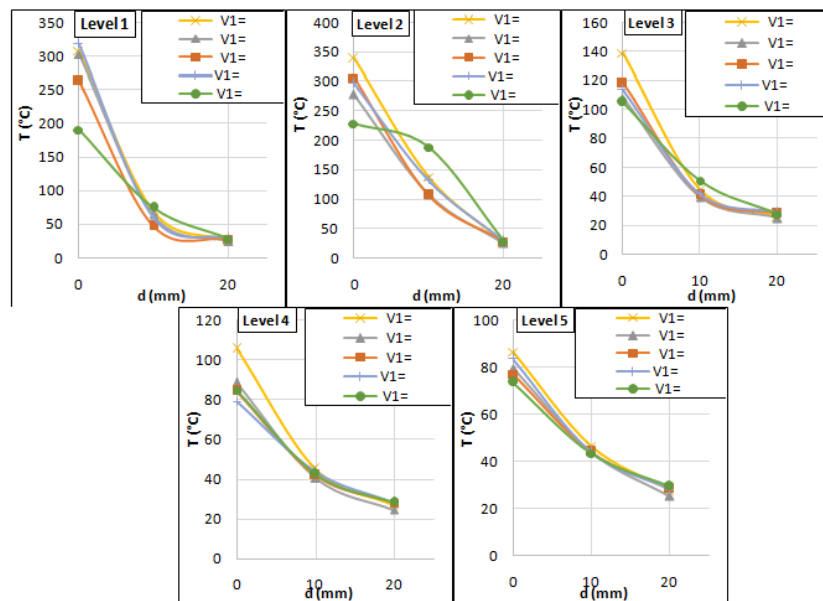


Fig 7: the effect of changing the secondary air velocity on temperature profile at fixed primary air velocity ($V_2 = 17.94$ m/s).

3.2Lift off distance

There was no noticeable lift off distance between the flames and the burner, and the flame base was adherent to the burner. The flame stability is affected by the lift off distance, and when the flame was so close to the burner, the flame became more stable, but the burner got hot, which accords with Turns[14].

3.3Flame length and width

The flame length varies according to the air velocity provided by primary and secondary air

pipes since the fuel flow rate remains constant throughout the experiment. The photo processing with MATLAB is summarized in Tables 2, 3and4. Figure 8-a shows that the flame length was affected by supplying secondary air with various velocities to the combustion zone and the maximum flame length is 7.82 cm at $V_1= 0$ and $V_2= 16.5$ m/s. Figure 8-b shows that the flame width was affected by adding secondary air with various velocities to the combustion zone and the maximum flame width is 3.01cm at $V_1= 18.03$ m/s and $V_2= 17.94$ m/s.

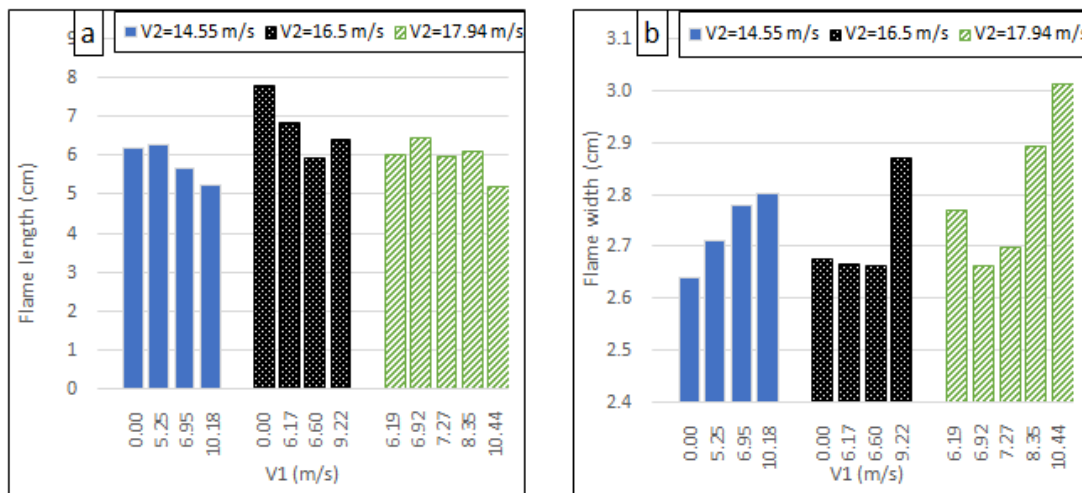


Fig 8: (a) flame length and (b) flame width at constant primary air velocity (V_2) and various secondary air velocities (V_1).

Table 2: image processing summary at $V_2= 14.55$ m/s.

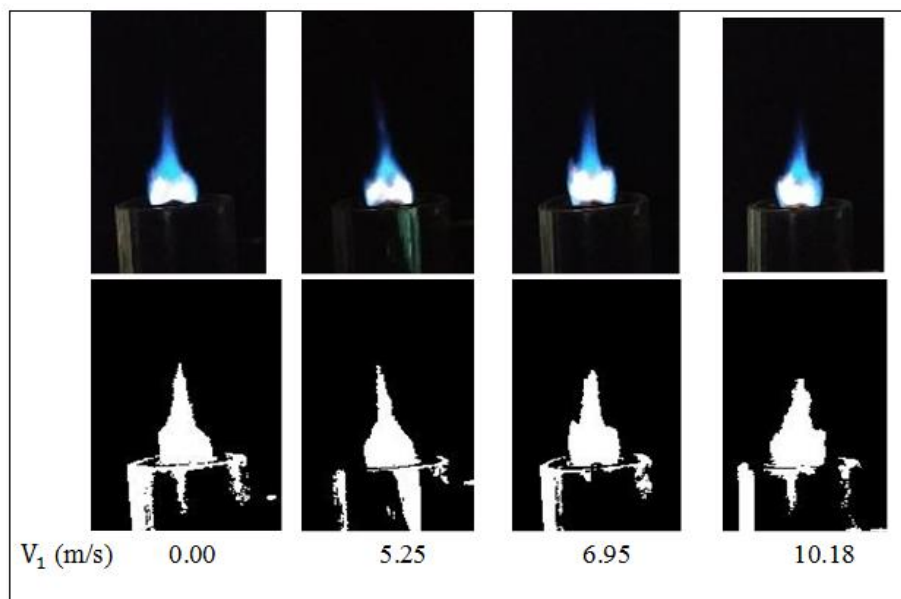


Table 3: image processing summary at $V_2= 16.5$ m/s.

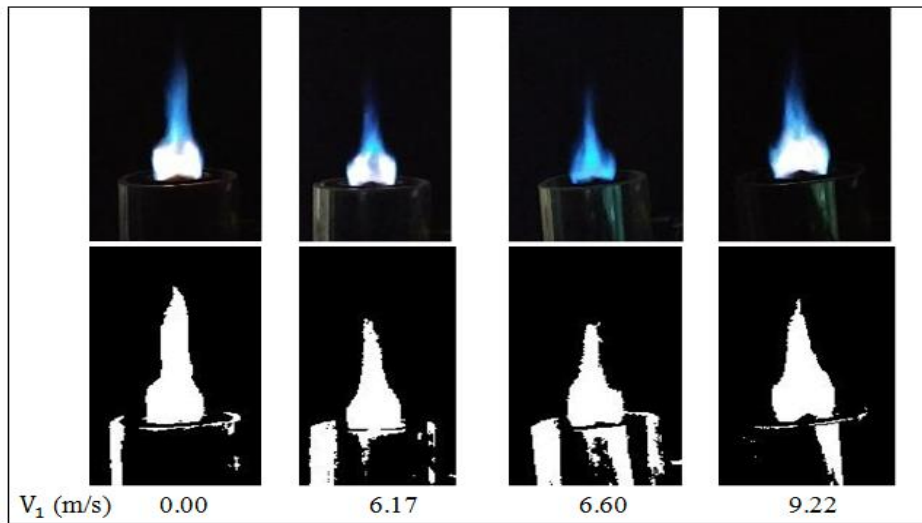
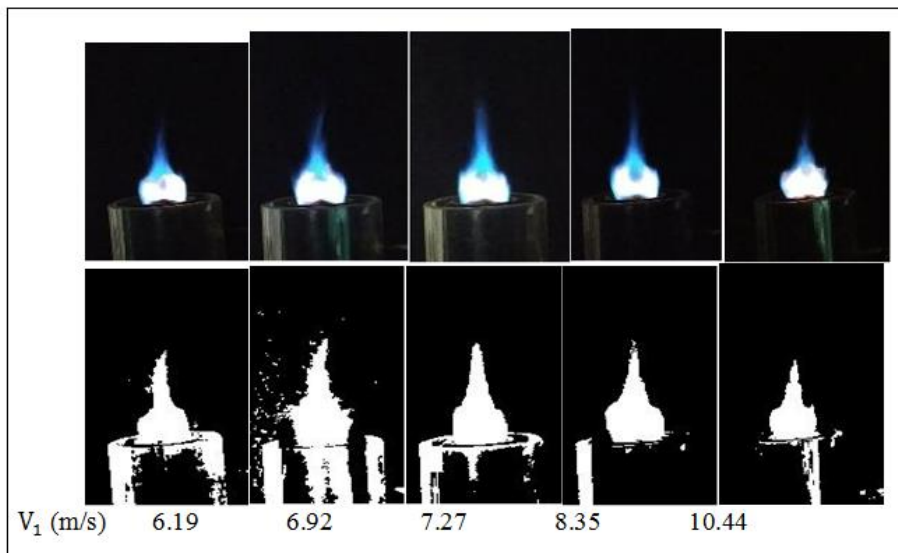


Table 4: image processing summary at $V_2= 17.94$ m/s.



3.4 Emissions

Figure 9 shows CO and NO_x concentrations at constant primary air velocity (V_2) with various secondary air velocities (V_1). It shows that the maximum concentration of CO is 1211 ppm at

$V_1= 6.6$ m/s and $V_2= 16.5$ m/s and the minimum concentration of CO is 584 ppm at $V_1= 10.18$ m/s and $V_2= 14.55$ m/s. NO_x emissions did not exceed 3 ppm throughout the experiment.

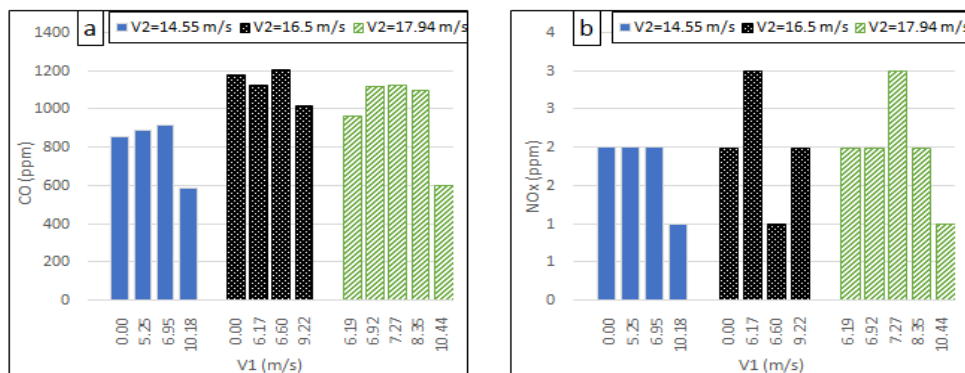


Fig 9: (a) CO and (b) NO_x concentrations at constant primary air velocity (V_2) with various secondary air velocities (V_1).

4. Conclusion

- The flame structure, flame length, and flame width are all affected by the air speed entering the combustion zone.
- The developed flame holder resulted in eliminating the flame lift off distance which improve the flame stability, but the flame holder became overheated.
- Supplying secondary air affected the flame temperature at the measuring points.
- The highest temperatures were at velocities of ($V_1 = 9.22$ m/s, $V_2 = 16.5$ m/s) and at ($V_1 = 6.6$ m/s, $V_2 = 16.5$ m/s).
- When the primary air velocity was constant $V_2 = 14.55$ m/s and the secondary air velocity varied, flame heights decreased and flame width increased with the increase of secondary air velocity.
- NO_x concentrations were low and did not exceed 3 ppm.
- CO concentrations varied with the variation of secondary air velocity.

References

- [1] Sara McAllister, Jyh-Yuan Chen, A. Carlos Fernandez-Pello, Fundamentals of Combustion Processes, Springer Science+Business Media, LLC, 2011.
- [2] Yunus A. Çengel, Michael A. Boles, Thermodynamics: an engineering approach, eighth edition, McGraw-Hill Education, 2015.
- [3] Haodong Zhang, Xi Xia, Yi Gao, "Instability transition of a jet diffusion flame in quiescent environment," *Proceedings of the Combustion Institute*, vol. 38, no. 3, pp. 4971-4978, 2021.
- [4] Anil R. Kadam, Ritesh Kumar Parida, Vijaykumar Hindasageri, G.N. Kumar, "Heat transfer distribution of premixed methane-air laminar flame jets impinging on ribbed surfaces," *Applied Thermal Engineering*, 2019.
- [5] Muhammad Mushahid Rafique Qureshi, Chao Zhu, "Crossflow evaporating sprays in gas-solid flows: Effect of aspect ratio of rectangular nozzles," *Powder Technology*, vol. 166, no. 2, p. 2006, 60-71.
- [6] Chunde Yao, Peilin Geng, Zenghui Yin, Jiangtao Hu, Dalu Chen, Yusheng Ju, "Impacts of nozzle geometry on spray combustion of high pressure common rail injectors in a constant volume combustion chamber," *Fuel*, vol. 179, pp. 235-245, 2016.
- [7] M. Henriksen, A.V. Gaathaug, J. Lundberg, "Determination of underexpanded hydrogen jet flame length with a complex nozzle geometry," *International Journal of Hydrogen Energy*, 2018.
- [8] Changchun Liu, Linyuan Huang, Tiandiao Deng, Shasha Zhou, Xinlei Liu, Jun Deng, Zhenmin Luo, "On the influence of nozzle geometry on jet diffusion flames under cross-wind," *Fuel*, 2019.
- [9] Toshio Mogi, Sadashige Horiguchi, "Experimental study on the hazards of high-pressure hydrogen jet diffusion flames," *Journal of Loss Prevention in the Process Industries*, vol. 22, no. 1, pp. 45-51, 2009.
- [10] G. Kalaghatigi, "Lift-off heights and visible lengths of vertical turbulent jet diffusion flames in still air," *Combustion Science and Technology*, vol. 41, pp. 17-29, 1984.
- [11] Nirupama Gopaldaswami, Yi Liu, Delphine M. Laboureur, Bin Zhang, M. Sam Mannan, "Experimental study on propane jet fire hazards: comparison of main geometrical features with empirical models," *Journal of Loss Prevention in the Process Industries*, vol. 41, pp. 365-375, 2016.
- [12] Tomohiko Imamura, Shota Hamada, Toshio Mogi, Yuji Wada, Sadashige Horiguchi, Atsumi Miyake, Terushige Ogawa, "Experimental investigation on the thermal properties of hydrogen jet flame and hot currents in the downstream region," *International Journal of Hydrogen Energy*, vol. 33, no. 13, pp. 3426-3435, 2008.
- [13] Zhirong Wang, Kewei Jiang, Kun Zhao, Pinkun Guo, "Macroscopic characteristics and prediction model of horizontal extension length for syngas jet flame under inclined conditions," *International Journal of Hydrogen Energy*, vol. 46, no. 44, pp. 23091-23099, 2021.
- [14] Stephen R. Turns, An introduction to combustion : concepts and applications, third edition, McGraw-Hill Companies, 2000.
- [15] Halleh Mortazavi, Yiran Wang, Zhen Ma, Yang Zhang, "The investigation of CO2 effect on the characteristics of a methane diffusion flame," *Experimental Thermal and Fluid Science*, vol. 92, pp. 97-102, 2018.